Turk J Elec Eng & Comp Sci
() : –
© TÜBİTAK

Multi-Kernel Embedded Fusion UNet (MKEF-UNet): A Robust Deep Learning Approach for Accurate Segmentation of Chagas Parasites

Preet Kumar[1]*, Carlos Brito-Loeza[2] , Lavdie Rada[3]
[1]Information Technology, Faculty of Engineering and Natural Sciences, Bahcesehir University, Istanbul, Turkey,
ORCID iD: https://orcid.org/0000-0003-1690-7056
[2]Mathematics, Computational Learning and Imaging Research, Universidad Autónoma de Yucatán, Merida , Mexico,
ORCID iD: https://orcid.org/0000-0003-2970-2113
[3] Biomedical Engineering, Faculty of Engineering and Natural Sciences, Bahcesehir University, Istanbul, Turkey,
ORCID iD: https://orcid.org/0000-0002-2688-4962

Received: .202 • **Accepted/Published Online:** .202 • **Final Version:** ..202

Abstract:
This paper introduces a noval approach for segmenting Chagas parasites on stained blood smear samples from mice during the acute phase of infection with *Trypanosoma cruzi* utilizing a U-Net-based deep learning model named Multi-Kernel Embedded Fusion UNet (MKEF-UNet). Our proposed model incorporates DenseNet-121 for feature extraction, a classifier module for predicting parasite information, and a segmentation decoder with multiscale feature fusion to generate precise segmentation results. Notably, the integration of the embedded vector module, multi-kernel convolutions with dilations, and advanced data augmentation techniques significantly enhance the model's robustness and generalization capabilities. In extensive experiments on the Chagas dataset, MKEF-UNet achieves state-of-the-art performance, attaining an Intersection over Union (IoU) of 0.8683 and a Dice score of 0.9189 on the test set. The paper provides a detailed exposition of the model's architecture, training methodology, and the employed loss functions. This research not only presents a novel segmentation approach but also underscores the model's superiority in accuracy and robustness through the incorporation of advanced features. By introducing robust components and techniques, MKEF-UNet surpasses previous methods, showcasing its potential as a promising solution for the detection and segmentation of Chagas parasites in real-world scenarios.

Key words: Chagas disease, Trypanosoma cruzi, Deep learning models, Image Segmentation

1. Introduction

Chagas disease, also known as American trypanosomiasis, is a significant health menace instigated by the protozoan *Trypanosoma cruzi* (*T. cruzi*) [1].This disease represents a substantial public health challenge, predominantly prevalent in Latin American nations, and affects millions of individuals worldwide WHO24. Epidemiological data suggests that Chagas disease impacts around 6 to 7 million individuals in Latin America, with an additional 300,000 cases identified in the United States and between 80,000 to 120,000 cases in Europe. In contrast, official records from Mexico report merely a few hundred cases annually. However, it is postulated that there are approximately 1.1 million individuals in Mexico infected with (*T. cruzi*), and a further 29.5 million are at potential risk of acquiring the disease [2]. The disease is typically transmitted via contact with the feces or urine of infected triatomine bugs [1], but can also be contracted through the oral consumption

*Correspondence: preetpanchani1@gmail.com of contaminated food, mother-to-child transmission, blood transfusion, organ transplantation, and laboratory accidents [3–5].

Chagas disease consists of an acute and a chronic phase. The acute phase transpires within 6 to 8 weeks after infection and is marked by high levels of parasitemia in the bloodstream [6, 7]. The chronic phase, manifesting 5 to 15 years later, lasts for the infected individual's lifetime and features intracellular parasites forming pseudo-nests in the heart and digestive muscles WHO24. Timely diagnosis is crucial, as Chagas disease can be cured if treatment is initiated during the acute phase. Microscopic examination of fresh blood or stained blood slides is considered quickest and most cost-effective method to diagnose Chagas disease during the acute phase [8–12]. However, laboratory diagnosis has some limitations: it requires trained microscopists to observe the parasites, which can lead to errors and heterogeneity, manual search and identification of parasites is time-consuming, delaying laboratory results and treatment initiation, and methods enhancing parasite search in microscopic images can be expensive and prohibitive for low-income settings [1, 13].

To address the pressing need for accurate and efficient diagnosis of acute Chagas disease, machine learning (ML) algorithms offer a promising solution by automating the search and detection of parasites, thereby enhancing image analysis reproducibility [14, 15]. This approach has been successfully employed in related studies on parasitic infections, such as the detection of Plasmodium ssp., the causative agent of malaria, using machine learning techniques [16, 17]. Despite the significant threat posed by Chagas disease to populations in endemic areas, there is a noticeable lack of deep learning-based research focused on providing healthcare systems with efficient and automated methods for detecting or segmenting the (*T. cruzi*) parasite observed in blood sample images. Such advances would enable patients to receive timely medical treatment, mitigating the impact of this potentially life-threatening disease [18, 19]. notable strides in the field of classification, the segmentation task continues to pose significant challenges, with achieving high accuracy proving particularly elusive. This research addresses the persistent difficulty in obtaining precise segmentations for the detection of the (*T. cruzi*) parasite in blood sample images. Recognizing the critical need for accurate segmentation in this context, our primary objective is to advance the state-of-the-art by introducing an robust approach.

This study introduces a novel segmentation methodology, embodied in the Multi-Kernel Embedded Fusion UNet (MKEF-UNet), which not only presents a paradigm shift but also establishes its superiority in terms of accuracy and robustness. The incorporation of advanced features, such as the embedded vector module, multi-kernel convolutions with dilations, and strategic data augmentation techniques, contributes to MKEF-UNet's remarkable performance.

By surpassing the limitations of previous methods, MKEF-UNet emerges as a promising solution for the detection and segmentation of Chagas parasites in real-world scenarios. This research not only highlights the immediate implications for improved diagnostics but also sets the stage for enhanced methodologies in broader medical imaging applications.

The rest of this paper is structured as follows: The previous works is in Section 2, Section 3 details the materials used and all machine learning, deep learning techniques and data pre-processing used in our study. In Section 4, we present the experimental work and results obtained with different models, highlighting the best model. Section 5 concludes the paper with a brief discussion of our findings.

2. Previous Work

Detecting Chagas parasites in blood sample images has been a subject of interest for researchers for over a decade, resulting in the development of numerous algorithms and techniques to accurately identify parasites through classification. Initially, research focused on feature extraction and classical machine learning models. In recent years, deep learning techniques have emerged as a promising approach. In this section, we provide an overview of the evolution of these methods, highlighting their strengths and limitations, and offering context for our proposed solution. However, achieving accurate segmentation to indentify the (*T. cruzi*) parasite in blood sample images remains a challenging task with limited research, as we will outline in the upcoming summary.

In 2013, Soberanis-Mukul et al. [20] proposed an computerized method for detecting Chagas disease using a combination of segmentation and classification techniques. The method involved pre-processing raw images to remove noise and unwanted features, followed by binary segmentation employing a Gaussian model, which calculated the likelihoods based on the Bayesian framework to identify clusters of pixels potentially representing a parasite. Subsequently,the partitioned images were subjected to categorization using a pre-configured K-Nearest Neighbors (KNN) classifier, as described in Peterson et al. [22]. This classifier was trained to achieve a binary classification, distinguishing between images containing the (*T. cruzi*) parasite and those without it. The algorithm, tested against a dataset of 120 images, achieved a sensitivity of 0.98 and a specificity of 0.85. However, the authors acknowledged the need for improvements in false negative and true positive rates and cited limitations such as a smaller training dataset and the requirement of a non-fixed threshold value for accurate parasite classification.

In 2014, Soberanis-Mukul [21] conducted a study that compared three classifiers - SVM, AdaBoost, and ANN - to segment (*T. cruzi*) parasites. The study was divided into three stages - computing superpixels, optimal feature extraction, and classifier training employing ANN with error backpropagation, AdaBoost with perceptron ensemble, and SVM. The researchers utilized superpixels, which represent clusters of pixels within an image that represent continuous regions, to aid in neighborhood-aware feature extraction. During the experiment, the performance of the three classifiers was compared to that of established classifiers, namely the Gaussian and Bayes Classifiers. The results revealed that the Gaussian method exhibited the smallest mean square error of 0.18568, succeeded by the SVM with an error of 0.22635, and the ANN model with an error of 0.361. Consequently, the researchers concluded that the Gaussian classifier performed better than the other classifiers in detecting and segmenting (*T. cruzi*) parasites.

In the 2015 study by Uc-Cetina et al. [23], the authors conducted a comparative analysis of two classification methodologies, namely AdaBoost and Support Vector Machine (SVM), with the objective of identifying the (*T. cruzi*) parasite in blood sample images. The researchers put forth a two-step algorithm, commencing with the learning of a binary AdaBoost classifier. The training was facilitated by the extraction of features utilizing Haar templates, specially tailored to the distinctive morphology of the (*T. cruzi*) parasite. Subsequently, a post-processing stage was implemented, deploying an SVM classifier with the intent of eliminating false positives. The amalgamation of AdaBoost and SVM methodologies demonstrated superior performance when compared with the standalone SVM algorithm. The combined approach yielded a sensitivity metric of 100% and a specificity metric of 93.25%. This investigation underscores the effectiveness of machine learning methods in detecting Chagas parasites and the importance of considering shape, color, and texture features for accurate detection. While the AdaBoost method offers faster computation due to the integral images trick, the authors acknowledge the limitations of time-consuming image segmentation and emphasize the need for rapid processing in applications requiring swift scanning of numerous images.

Pereira et al. [24], in 2019, introduced a deep learning algorithm for Chagas parasite classification, potentially the first of its kind in the literature. They employed a pre-trained MobileNetV2 model for feature extraction, succeeded by a meticulously adjusted single-neuron dense layer. The approach achieved 96.4%

accuracy, 95.4% precision, 97.6% sensitivity, and a 96.5% F1-score on the validation dataset. However, the test accuracy was only 72% due to overfitting and limited dataset size, as noted by the authors. This raises concerns regarding the model's effectiveness in real-world applications.

In 2020, Allan Ojeda-Pat et al. [25] introduced a deep learning technique for the automated identification of (*T. cruzi*) parasites in blood specimen images, aiming to accelerate the diagnosis of Chagas disease and provide an alternative to manual visual inspection. The authors deployed a convolutional neural network, built on U-Net architecture, and trained it using a range of loss functions to ensure reliable outcomes. The application of the Weighted Binary Cross-Entropy Loss function led to the highest F2 score and recall values, culminating in an F2 score of 80%, a recall of 87%, a precision of 63%, and a Dice score of 68%, thereby demonstrating the potential of deep learning approaches in enhancing diagnostic accuracy and efficiency.However, the study's limitations include a highly imbalanced dataset, a simple U-Net architecture instead of more efficient and robust models, and a small test set, potentially affecting the model's robustness.

In 2021, Diogo Silva et al. [26] developed a machine learning approach using a random forest (RF) algorithm to detect and count (*T. cruzi*) trypomastigotes in micrographs taken by a 12-megapixel mobile device camera. They extracted morphometric, color, and texture features from 1,314 parasites and achieved a precision of 87.6%, a sensitivity of 90.5%, and an area under the ROC curve of 0.942. Despite its promising performance, there are limitations, such as reliance on lower-resolution images, a relatively small test dataset, and untested comparisons to deep learning approaches. Furthermore, the RF algorithm's performance is influenced by mobile phone cameras limitations, such as object outline and image sharpness. Higher false-positive rates occurred in regions with leukocytes and higher cell density, and increased false-negative rates in regions with lower contrast and sharpness.

The most recent work related to the segmentation task was published on 2022, by Allan Ojeda-Pat et al. [27]. The authors proposed an effective residual convolutional neural network, named Res2Unet, specifically engineered for the semantic segmentation of (*T. cruzi*) parasites in blood sample images. Drawing inspiration from Heun's method for resolving ordinary differential equations, Res2Unet incorporates active contour loss and enhanced residual connections. The model was trained on 626 blood sample images and was subsequently evaluated on a test set of 207 images. It achieved a Dice coefficient score of 84%, a precision of 85%, and a recall of 82%, thereby outperforming prior methodologies. The authors compared Res2Unet performance using various loss functions against other models, such as U-Net and ResUnet. However, they acknowledged limitations in their study, including a limited number of positive training examples and a smaller test set, which raise concerns about the effectiveness of their approach in large-scale, real-world applications.

Chagas parasite detection has progressed significantly, with methods transitioning from traditional machine learning to advanced deep learning techniques. However, further advancements in accuracy, speed, and robustness are necessary for practical, large-scale applications. We propose a novel approach using DenseNet121 [28] as an Encoder for feature extraction, followed by a classifier to predict information such as the number of parasites and pixels associated with each class. A decoder-encompassing features fusion technique also uses embedded vectors from the classifier module to efficiently segment the Chagas parasites. Our model has achieved state-of-the-art outcomes on the Chagas dataset, with an IOU of 0.8683 and a Dice score of 0.9189 on the test set. This reflects improved accuracy and robustness, highlighting its potential as a promising solution for detecting and segmenting Chagas parasites in real-world scenarios.

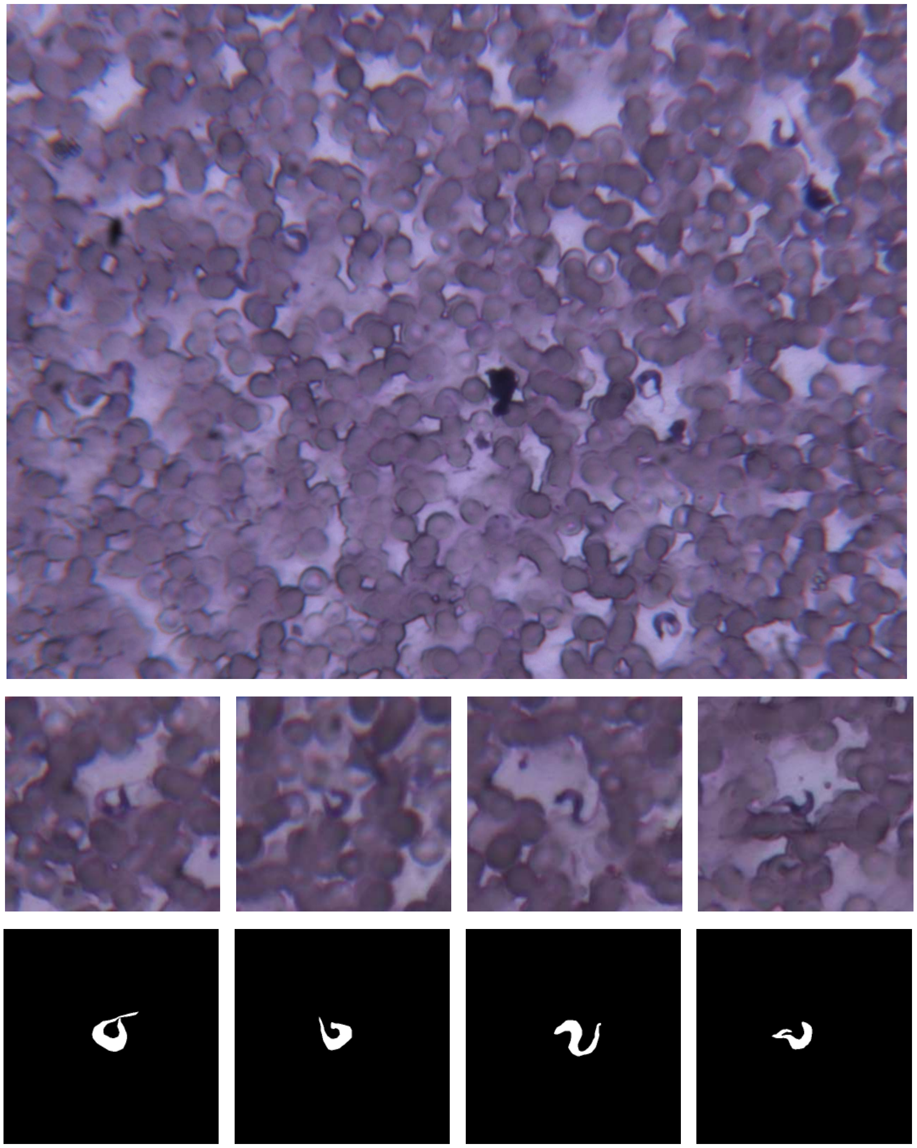

Figure 1: Original microscopic image in the first row, followed by parasite and mask ROIs in the second row and third row respectively.

3. Methodology

In this study, we propose a novel deep-learning model, MKEF-UNet, for segmentation tasks. This section describes the methodology used in the research, including dataset preparation, model architecture, and training process.

3.1. Database and Dataset Preparation

The process of preparing stained blood smear samples from mice during the acute phase of infection with *T. cruzi* was conducted in the Zoonoses Laboratory at the Centro de Investigaciones Regionales (CIR) in Mexico. Images of these samples were acquired using a Nikon Eclipse E600 optical microscope equipped with a camera offering a resolution of 75 dpi and dimensions of 2560 × 1920 pixels. Subsequently, 1,983 regions of interest

(ROIs) were extracted from the original images to establish the final image database, with a resolution of 512×512 pixels for each ROI, using the Python language. Within this database, 940 ROIs were identified as parasites, while 1,043 ROIs were classified as non-parasites (refer to Fig. 1 for visualization of the samples).

The provided dataset encompasses images in their original state before undergoing any data augmentation techniques. Data augmentation was implemented in real-time during the training phase. The dataset is categorized into three distinct groups: the training set consists of 1183 images, while both the validation and test sets contain 400 images each.

To train and evaluate the model, we process the input images and their corresponding masks. Input image-mask pairs were resized to a fixed dimension of 256 x 256 pixels. Additionally, we convert the mask data into numerical information by computing the number of Chagas and pixels associated with each class and normalizing it within the 0 to 1 range. The mask data is also converted into a one-hot encoding format to be used for loss computation.

3.2. Data Augmentation

Data augmentation is a powerful technique employed to amplify the number of images in the training dataset. This is accomplished by utilizing various image modifications like flipping (both horizontally and vertically), rotation, zooming, cropping, and translation to the original images. Additional augmentation techniques encompass sharpening, blurring, color space transformations, and region deletion.These techniques serve to diversify the dataset, thereby mitigating overfitting and enhancing the efficiency of the segmentation model.

In our approach, data augmentation is not only a foundational step but also a critical component throughout the training process. We begin by applying traditional image modifications to the original images, such as rotation (limited to 35 degrees), horizontal and vertical flipping, and coarse dropout. These initial augmentations are designed to diversify the dataset and prepare it for more effective learning. Examples of these augmented images are depicted in Figure 2

Subsequently, we further enhance the training process by generating an augmented version of the original image through additional horizontal and vertical flips. This results in pairs of images—each consisting of the originally augmented image and its further flipped counterpart. We process these pairs of images simultaneously with our model. This dual-input approach allows the model to learn from both the original image (which has already undergone initial augmentations) and its further altered version, thereby enabling a more comprehensive and effective learning experience.

A crucial aspect of our methodology is the application of inverse transformations to the predictions made on these further augmented images. Once the model predicts on these images, we apply an inverse transformation to realign these predictions with the orientation of the original images. This step is integral to our dual-loss computation technique, which calculates loss based on both the original and inversely transformed augmented images. This strategy significantly refines the model's parameters, enhancing its ability to generalize across various image orientations and styles.

3.3. Hyperparameters

In the course of our experiment, we carefully adjusted a range of hyperparameters to optimize our models for image segmentation task.The parameters, applied to the model, included an starting learning rate of 1e-4 and the Adam optimizer, known for its effectiveness in handling sparse gradients in complex scenarios. We also selected a modest batch size of 2 and set the training duration for 50 epochs. The Rectified Linear Unit (ReLU)

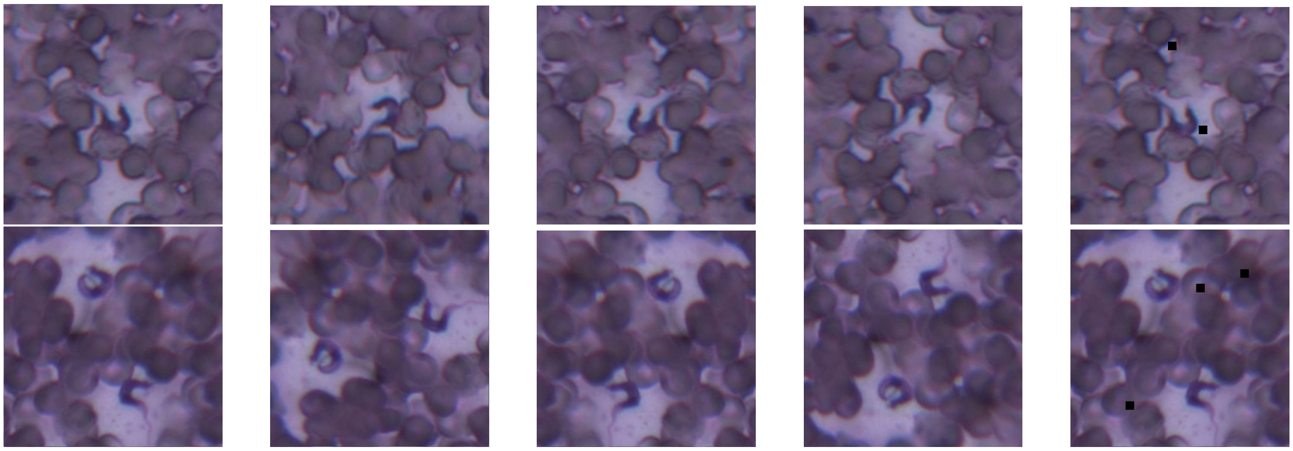

(a) Original Image (b) Rotated Image (c) Horizontal Flip (d) Vertical Flip (e) Coarse Dropout

Figure 2: Augmented images with rotation, horizontal flip vertically flipped and coarse dropout.

was chosen as the activation function, given its demonstrated success in deep learning contexts.Additionally, we implemented the ReduceLROnPlateau learning rate scheduler with a patience of 5 epochs to dynamically adjust the learning rate based on the monitored validation loss.

3.4. Model Architecture

The MKEF-UNet model, as shown in Figure 3, is an end-to-end deep learning model, a U-Net architecture, for Chagas parasite segmentation. The architecture consists of an encoder, a classifier, multi-kernel convolutions with dilations, multiscale feature fusion, and a segmentation decoder. The architecture is designed to capture both global and local contextual information from input images and produce highly accurate segmentation results.

3.4.1. Encoder

The encoder is based on DenseNet-121, a well-established backbone for feature extraction. The encoder has four output levels, each with a reduced feature channel count. We apply pointwise convolution to reduce the feature channels of the encoder to 96, which notably diminishes the number of parameters and accelerates the training process.

3.4.2. Classifier and Embedded Vector Module

The embedded vector module, as shown in Figure 4, predicts the number of Chagas parasites and their embedded vector. It is designed with two parallel fully connected layers with ReLU activation functions, followed by linear layers for the final output. The primary function of this module is to process the features derived from the encoder. It generates embedded vectors, which are then fed into the decoder blocks. This process significantly enhances the segmentation results, providing a more accurate and detailed representation of the parasites in the image.

The operation of the classifier module begins with an adaptive average pooling operation, mathematically

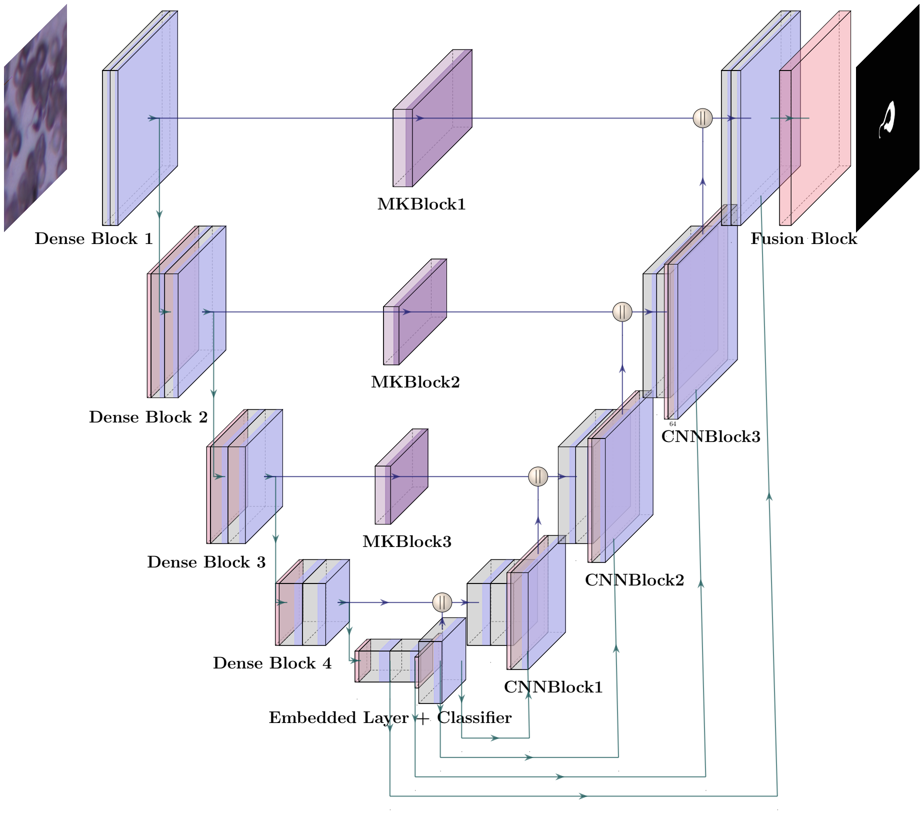

Figure 3: MKEF-UNet Model.

expressed as:

$$f_{ave}(X) = \frac{1}{N}\sum_{i=1}^{N} x_i \tag{1}$$

where X is the input feature map, N is the total number of elements in the pooling window, and x_i represents the i-th element within this window. Following the pooling operation, the pooled feature map is processed through fully connected layers as shown in equation 2. The operation of a fully connected layer is mathematically expressed as:

$$y_{jk}(z) = f\left(\sum_{i=1}^{n^H} W_{jk} z_i + W_{j0}\right) \tag{2}$$

where W is the weights matrix, z is the input(pooled feature map), W_{j0} is the bias term, n^H represents the total number of input features from the previous layer H to the current fully connected layer and f is a non-linear function, such as ReLU. This operation is applied to the output from the classifier module.

3.4.3. Multi-Kernel Convolutions with Dilations Module

This module, as shown in Figure 5, is employed to process the features extracted by the encoder at different scales. It employs dilation, a technique that increases the receptive field of the convolution layers, thus enabling

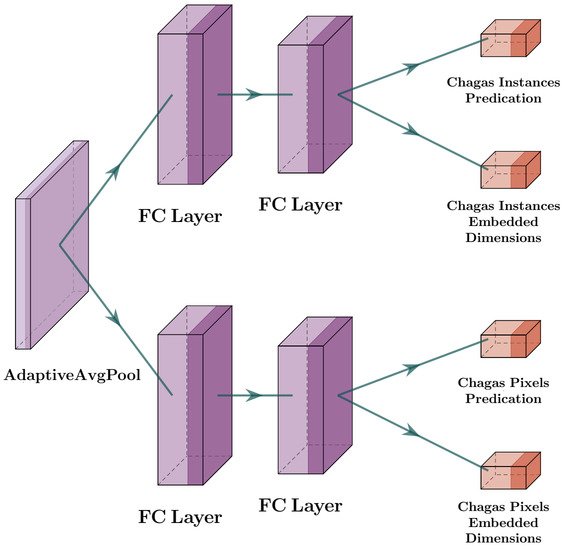
AdaptiveAvgPool
FC Layer
FC Layer
Chagas Instances Predication
Chagas Instances Embedded Dimensions
FC Layer
FC Layer
Chagas Pixels Predication
Chagas Pixels Embedded Dimensions

Figure 4: Classifier and Embedded Vector Module.

the model to incorporate a larger context without necessitating an increase in the number of parameters. This approach ensures computational efficiency while maintaining a comprehensive representation of the input data.

Moreover, the module is characterized by its use of multiple dilated convolutional layers with diverse kernel sizes, specifically 1, 3, 7, and 11. This strategic design choice allows the model to capture a wide range of spatial information, thereby enhancing its ability to detect and classify features of varying sizes and complexities.

In addition to these design elements, the module incorporates channel and spatial attention mechanisms. These mechanisms are designed to emphasize important features, allowing the model to assign varying levels of importance to different features. This selective focus on the most pertinent features significantly enhance the model's performance, equipping it with the capability to make more accurate and robust predictions. The mathematical expression for the dilated convolution operation in this module can be represented as:

$$f_k(x) = \sum_{d=1}^{D} W_k^d(x), k > 1 \tag{3}$$

where k is the kernel size, d is the dilation rate, and D is the maximum dilation rate.

3.4.4. Segmentation Decoder

The decoder module combines the multi-kernel dilated convolution features with the embedded classifier output to produce the final segmentation mask. It consists of three decoder blocks, each with upsampling layers, residual blocks, and element-wise addition of the embedded vector for the predicted number of Chagas instances. The decoder blocks receive input from the multi-kernel dilated convolution layers and progressively refine the segmentation output.

3.4.5. Multiscale Feature Fusion Module

This module, as shown in Figure 6, is responsible for fusing features from different scales in the decoder. It uses upsampling, concatenation, and convolutional layers to combine the features and generates a final multiscale

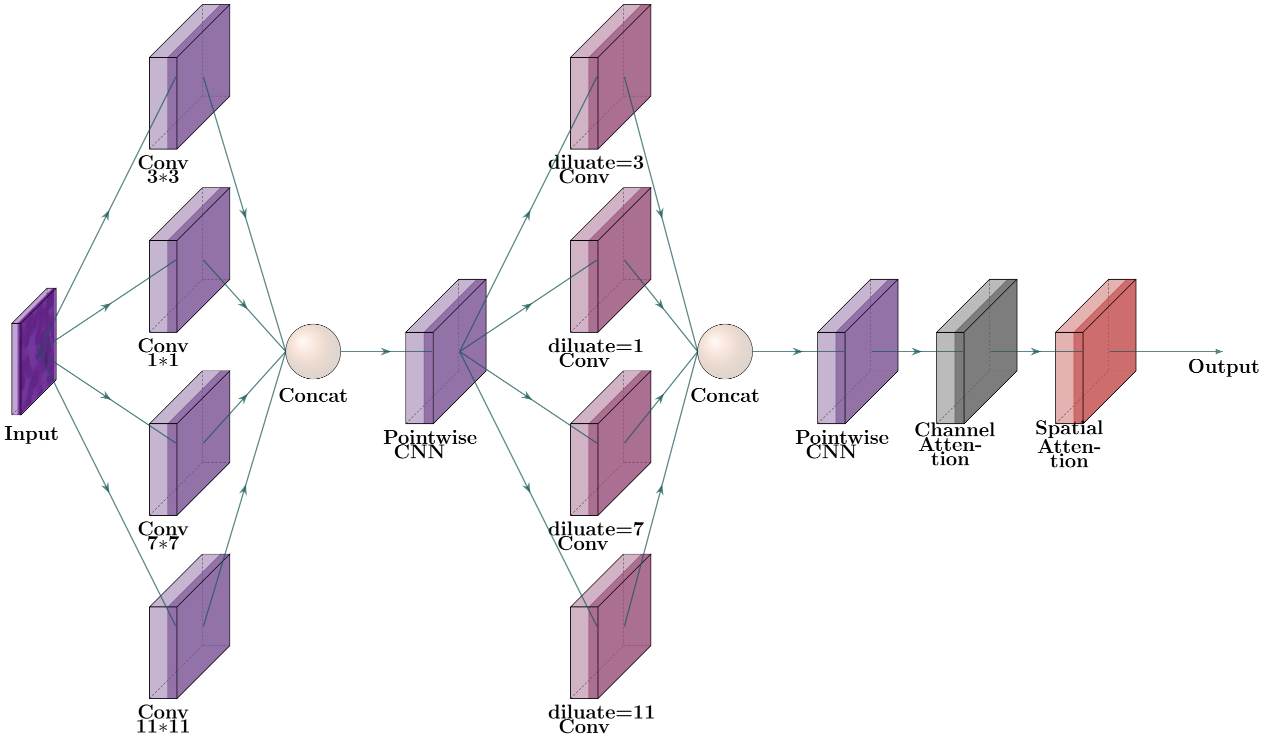

Figure 5: Multi-Kernel Diluation Module.

feature map for segmentation. Channel and spatial attention mechanisms are employed to further enhance the fusion process. The multiscale feature fusion can be mathematically expressed by equation 4 and 5:

$$F_{concat} = \text{Concatenate}(U(f_1), U(f_2), \ldots, U(f_n)) \tag{4}$$

$$y_{fusion} = Conv(F_{concat}) \tag{5}$$

where f_i represents the feature map at scale i, U is the upsampling operation, $Conv$ represents the convolution operation, and y_{fusion} is the output of the multiscale features fusion module.

3.4.6. Segmentation Output Module

The final segmentation output is generated using a 1x1 convolutional layer applied to the multiscale feature map. This layer produces a single-channel output representing the likelihood of every pixel belonging to the Chagas parasite class.

In summary, the model leverages a DenseNet-121 encoder, a classifier module, multi-kernel dilated convolutions with attention mechanisms, a segmentation decoder, and multiscale feature fusion to effectively segment Chagas parasites in the input image. The architecture is designed to capture multiscale information, fuse features from different levels, and incorporate classification information for improved segmentation performance.

3.5. Training Procedure

This sub section describes the system configurations, training and loss functions used in the research.

Algorithm 1 MKEF-UNet for Chagas Parasite Segmentation

```
Require: Image (input image for Chagas parasite segmentation)
Ensure: Segmentation Mask (binary mask indicating Chagas parasites) , NumOfChagasInstances
Procedure MKEF-UNet(Image)
  Initialize Model Components:
    Encoder(DenseNet-121)
    Classifier with Embedded Vector Module
    MultiKernelDilatedConv Module
    Decoder Blocks
    Multiscale Feature Fusion Layer
    Segmentation Output Layer

  Encoder Forward Pass:
    FeatureMaps ← DenseNet121_Encoder(Image)

  Classifier Embedded Module Forward Pass:
    NumOfChagasInstances, EmbeddedVectors ← ClassifierEmbeddedModule(FeatureMaps[-1])

  MultiKernelDilatedConv Forward Pass:
    EnhancedFeatureMaps ← MultiKernelDilatedConv(FeatureMaps)

  Decoder Blocks Forward Pass:
    Initialize DecodedFeatures as empty list
    for each level in EnhancedFeatureMaps do
      DecodedFeature ← DecoderBlock(level, EmbeddedVectors)
      DecodedFeatures.append(DecodedFeature)
    end for

  Multiscale Feature Fusion:
    FusedFeatures ← MultiscaleFeatureFusion(DecodedFeatures)

  Segmentation Output Generation:
    SegmentationMask ← Convolution(FusedFeatures, kernel_size=1)

  return SegmentationMask , NumOfChagasInstances
End Procedure
```

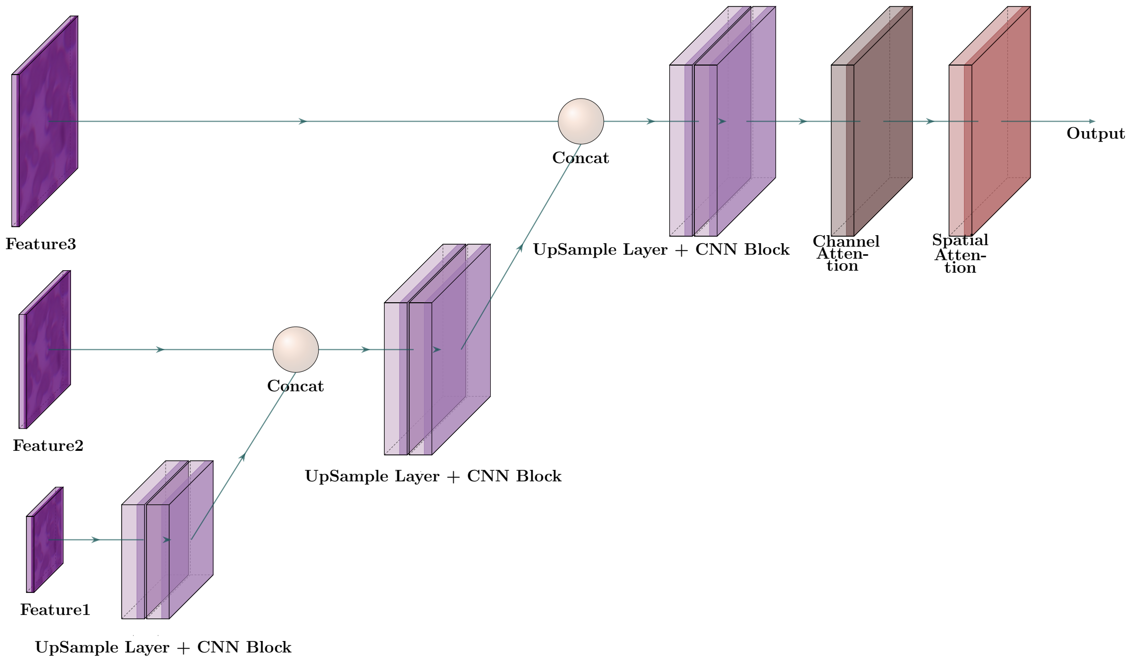

Figure 6: Features Fusion Module.

3.5.1. System Configuration and Dependencies

The experiments were conducted on a Windows 11 system equipped with an Intel Xeon processor running at 2.4 GHz, 8 GB RAM, 1 TB HDD, CUDA-enabled Nvidia GPU. The software environment consisted of Python, with Pytorch libraries as the backend. For GPU acceleration, CUDA and cuDNN dependencies were installed.

3.5.2. Model Training and Loss Functions

The training phase was executed over 50 epochs, leveraging the Adam optimizer for efficient learning. The training process was further optimized by dynamically adjusting the learning rate based on the validation loss, facilitated by the ReduceLROnPlateau learning rate scheduler. Three loss functions were employed to optimize the model's performance: (1) IoU Loss to compute the similarity between the ground truth and predicted masks; (2) Active Contour Loss to ensure smooth and accurate segmentation boundaries; and (3) Cross-Entropy Loss to classify the number of Chagas instances. During the training process, the model takes input images and produces segmentation masks and the number of Chagas instances. To enhance the model's robustness, data augmentation techniques are applied to the same images, which involve horizontal and vertical flips. The transformed images are then passed through the model to generate another set of predictions. The final loss is computed for both the original and transformed image predictions which are then used to refine the parameters of the model.

Moreover, after each epoch, the model's effectiveness was evaluated on the validation set using the IoU score. If the validation IoU score improved compared to the previous best score, the current model weights were saved. This ensured the retention of the model parameters that yielded the highest validation IoU, boosting the model's effectiveness on unseen data. This approach also provided a set of weights that can be used for other related tasks, enhancing the model's utility.

4. Experimental Results and Discussion

4.1. Evaluation Metrics

In this section, we discuss the evaluation metrics used to assess the performance of the proposed Chagas segmentation model. We will discuss their mathematical formulations and highlight key properties. The following evaluation metrics are employed in this study:

4.1.1. Weighted Cross-Entropy Loss

Weighted Cross-Entropy loss [29] is a modification of the standard Cross-Entropy loss, which assigns different weights to each class, addressing the issue of class imbalance in the dataset. The loss function is defined as:

$$L_{wCE}(y,\hat{y}) = -\sum_{i=1}^{N} w_i[y_i \log \hat{y}_i + (1-y_i)\log(1-\hat{y}_i)] \tag{6}$$

where w_i denotes the weight assigned to the i-th class, y_i represents the true label, and p_i is the predicted probability for that class.

4.1.2. Jaccard Loss

Jaccard loss [30], also referred to as Intersection over Union (IoU) loss, quantifies the similarity between two sets. It is defined as the proportion of the intersection to the union of the two sets:

$$L_J(A,B) = 1 - \frac{|A \cap B|}{|A \cup B|} \tag{7}$$

In the context of segmentation, A and B are the ground truth and predicted segmentation masks, respectively.

4.1.3. Dice Loss

Dice loss [31], also known as the Sørensen-Dice coefficient, is another measure of set similarity. It is defined as the harmonic mean of precision and recall, or equivalently, as twice the product of intersection and union divided by the sum of their sizes:

$$L_D(A,B) = 1 - \frac{2|A \cap B|}{|A| + |B|} \tag{8}$$

Similar to Jaccard loss, A and B represent ground truth and predicted segmentation masks, respectively.

4.1.4. Focal Loss

Focal loss [32] is a modification of Cross-Entropy loss designed to address the issue of class imbalance during training. By reducing the loss contribution from straightforward examples and concentrating on challenging examples, Focal loss enhances the learning of the minority class. The loss function is defined as:

$$L_F(y,\hat{y}) = -\sum_{i=1}^{N}[y_i(1-\hat{y}_i)^{\gamma}\log\hat{y}_i + (1-y_i)(\hat{y}_i)^{\gamma}\log(1-\hat{y}_i)] \tag{9}$$

where y_i indicates the true class label of the i^{th} example, with $y_i = 1$ for the positive class and $y_i = 0$ for the negative class. The parameter γ is a focusing parameter that scales the loss contribution of each example.

The modulating factors $(1-\hat{y}_i)^\gamma$ for the positive class and $(\hat{y}_i)^\gamma$ for the negative class serve to decrease the loss from easy examples (those predicted with high confidence) and increase it for hard examples, effectively emphasizing the learning on misclassified instances by the model.

4.1.5. Active Contour Loss

Active Contour Loss is a loss function designed for segmentation tasks that encourages smooth and coherent segmentation boundaries. It is inspired by the active contour model in image processing and combines region-based and boundary-based information. The loss function can be defined as:

$$L_{ACL} = \lambda L_{region} + (1-\lambda) L_{boundary}, \tag{10}$$

where λ is a weighting parameter, L_{region} is a region-based term that measures the similarity between the predicted segmentation mask and the ground truth, and $L_{boundary}$ is a boundary-based term that promotes the smoothness of the segmentation boundaries.

4.2. Experimental Results for the Model

In this study, we evaluate the effectiveness of our proposed model, we compared it withseveral existing models, including UNet, Res2Unet, ResUnet, Gaussian Method, and SVM. The comparison is based on key metrics like the Dice Score, F1 Score, Precision, and Recall, crucial for assessing the accuracy and reliability of segmentation models in identifying the *T. cruzi* parasite.

Our proposed model, MKEF-UNet, achieved a Dice Score of 0.9189, an F1 Score of 0.9253, a Precision of 0.9063, and a Recall of 0.9453, outperforming the other models by a significant margin, as it can be observed in Table 1.

From this table we can see that the Res2Unet and UNet models developed by Ojeda-Pat et al. [25, 27] showed relatively lower performance metrics. The Res2Unet model achieved a Dice Score of 0.84, an F1 Score of 0.83, a Precision of 0.85, and a Recall of 0.82, while the UNet model scored a Dice Score of 0.6825, an F1 Score of 0.7311, a Precision of 0.6304, and a Recall of 0.8702. These comparisons underscore the advanced capabilities of our MKEF-UNet model.

ResUnet model, a variant of the UNet architecture, achieved a Dice Score of 0.82, an F1 Score of 0.820, a Precision of 0.84, and a Recall of 0.80. Despite its better performance compared to the Gaussian and SVM methods, it was still outperformed by MKEF-UNet demonstrate its effectiveness in accurately segmenting the *T. cruzi* parasite.

The Gaussian Method and the SVM model showed significant limitations. The Gaussian Method achieved a Dice Score of 0.22 and an F1 Score of 0.223, indicating poor precision and accuracy in segmentation. The SVM model yielded even lower scores, with a Dice Score of 0.13 and an F1 Score of 0.130, suggesting its inadequacy for complex segmentation tasks like *T. cruzi*.

Furthermore, we trained our model for 50 epochs and monitored its performance on the training and validation sets using the Dice coefficient score and Jaccard score. Figures 7 show the learning curves for the Dice coefficient score and Jaccard score, respectively. The results indicated that our model performed well on both the training and validation sets, with the Dice coefficient score and Jaccard score improving as the training progressed. The training and validation loss values were also monitored during the training, and the active contour loss decreased consistently over the 50 epochs, as shown in Figure 7. As we can observe, this model performed very well without facing any overfitting problem.

Table 2 presents six columns with various different images, with the first three columns displaying accurate segmentation of both the Ground Truth and the proposed model, while the other three columns exhibit incomplete segmentation of the object of interest, despite successful segmentation of the parasite.

Table 1: Comparison of Our Model with Previous Works on *T. cruzi*

Reference	**Model**	**Dice Score**	**F1 Score**	**Precision**	**Recall**
Our Proposed Model	MKEF-UNet	0.9189	0.9253	0.9063	0.9453
Ojeda-Pat et al.[27]	Res2Unet	0.84	0.83	0.85	0.82
Ojeda-Pat et al.[27]	ResUnet	0.82	0.820	0.84	0.80
Ojeda-Pat et al.[25]	UNet	0.682	0.7311	0.6304	0.8702
Ojeda-Pat et al.[27]	Gaussian Method	0.22	0.223	0.13	0.80
Ojeda-Pat et al.[27]	SVM	0.13	0.130	0.07	0.94

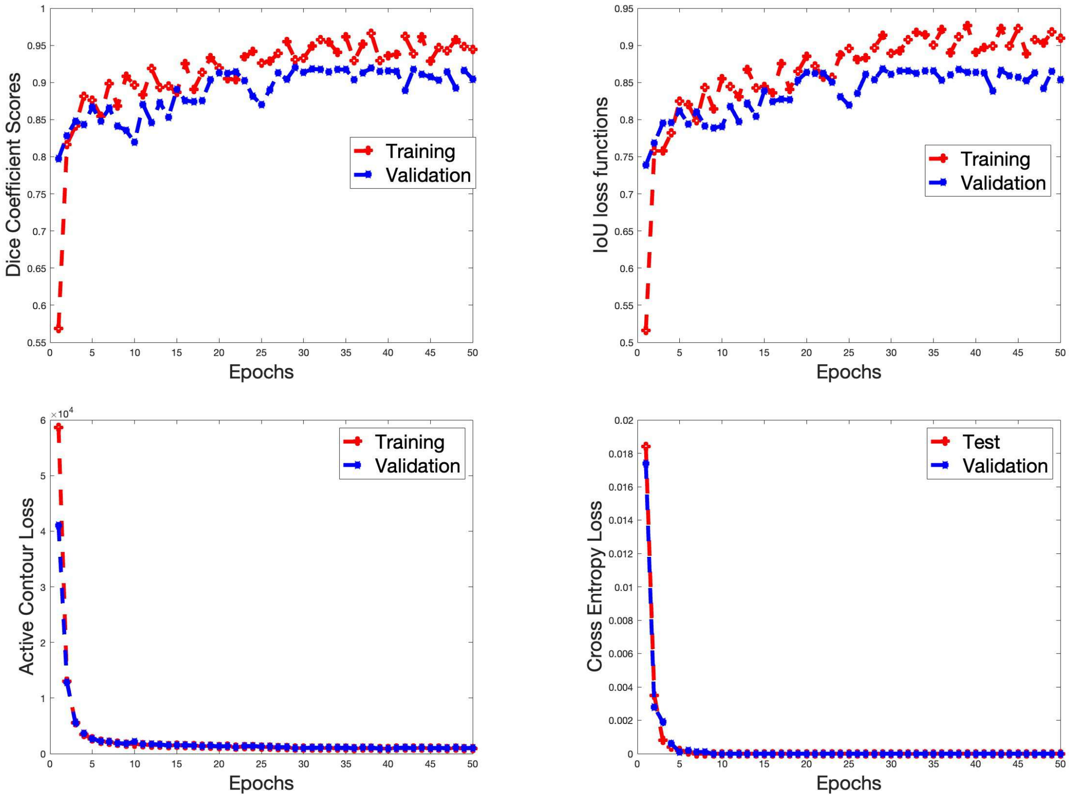

Figure 7: In the first row we show Dice coefficient scores for training and validation followed by IoU loss functions for the proposed model in 50 epochs experiment. The second row shows the model learning curve through the active contour loss and the cross entropy loss.

Ablation Study of MKEF-UNet: In our ablation study of the MKEF-UNet model, we strategically removed key components to assess their individual contributions to the model's performance in segmenting the *T. cruzi* parasite. The removal of the Classifier with Embedded Vector Module resulted in a decrease in the Dice Score from 0.9189 to 0.8987, highlighting its significant role in feature refinement and performance enhancement. Similarly, the exclusion of the MultiKernelDilatedConv Module led to a reduction in the Dice

Score to 0.8928, indicating its importance in feature integration across scales. Intriguingly, the ablation of the Multiscale Feature Fusion Layer showed a minimal impact, with the Dice Score marginally decreasing to 0.9162. This suggests that while this layer contributes to the model's performance, its role is not as critical as the other components in our segmentation task. These insights underline the importance of the Classifier with Embedded Vector and MultiKernelDilatedConv modules in the MKEF-UNet architecture.

Table 2: Comparison of images, ground truth, perfect predictions and missing predictions

Image	Ground Truth	Accurate Predictions	Image	Ground Truth	Missing Prediction
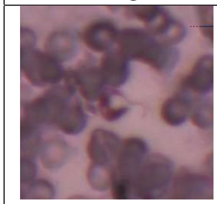	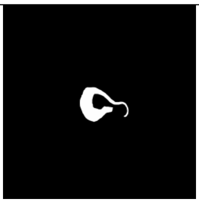	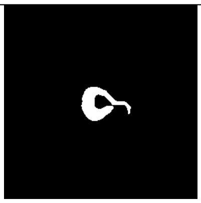	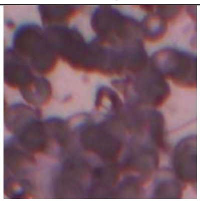	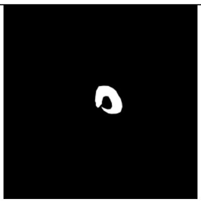	+ img/8f.pdf
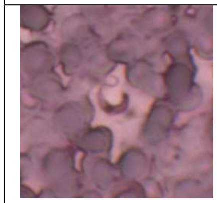	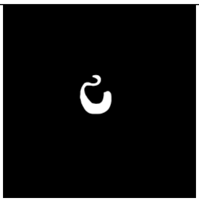	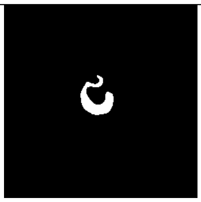	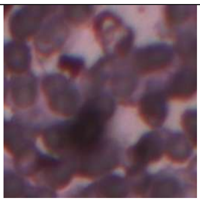	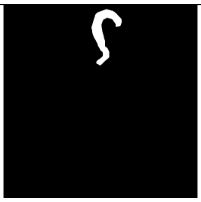	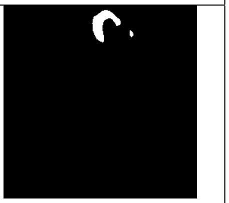
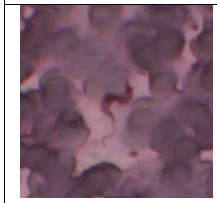	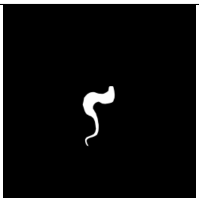	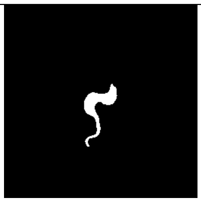	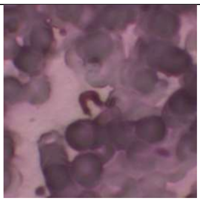	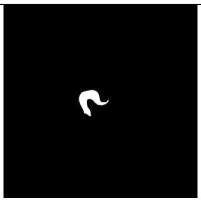	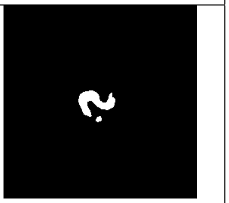
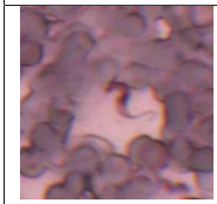	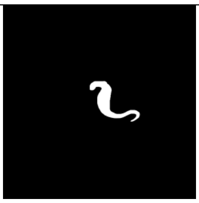	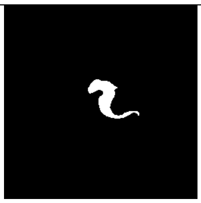	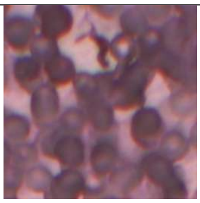	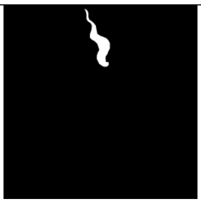	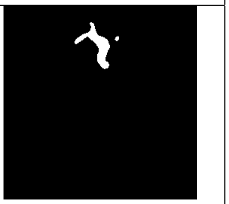
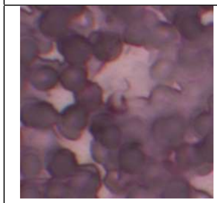	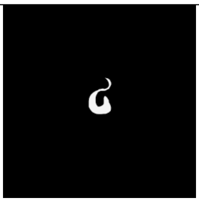	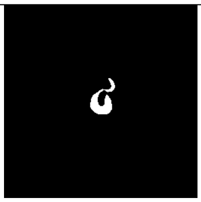	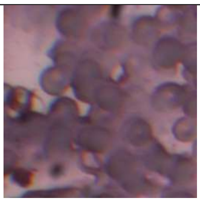	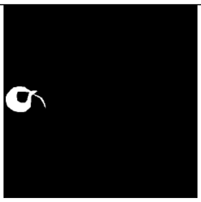	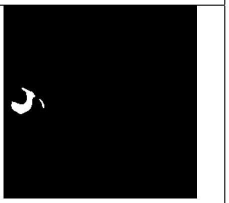
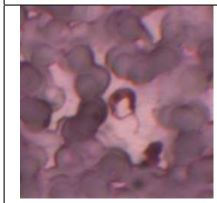	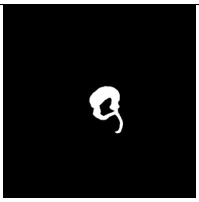	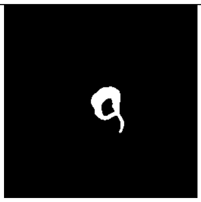	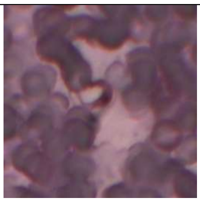	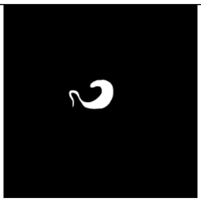	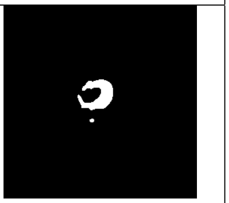

5. Conclusion

In this research, we have presented a novel approach, MKEF-UNet, for the segmentation of Chagas parasites using a U-Net based deep learning model. Our model incorporates DenseNet121 for feature extraction, a classifier module for predicting parasite information, and a segmentation decoder with multiscale feature fusion to generate accurate segmentation results. The introduction of the embedded vector module, multi-kernel convolutions with dilations, and comparing the similarity of the model's prediction on the original and transformed image pair have significantly improved the model's robustness and generalization capabilities.

The proposed model has achieved state-of-the-art performance on the Chagas dataset, with an IOU of 0.8683 and a Dice score of 0.9189 on the test set. These results indicate an improvement in accuracy and robustness compared to previous methods, highlighting the potential of our approach as a promising solution for detecting and segmenting Chagas parasites in real-world scenarios.

Future work could focus on exploring other advanced feature extraction techniques, refining the classifier module for more precise parasite information prediction, and optimizing the segmentation decoder for better performance. Additionally, the model's robustness could be further tested by applying it to datasets with varying image quality, resolution, and staining techniques, which are common challenges in real-world diagnostic settings. This would give a thorough comprehensive understanding of the model's operational efficiency and its readiness for deployment in clinical environments. Furthermore, the model could be adapted for the segmentation of other biomedical images, thus expanding its applicability in the field of medical image analysis.

Acknowledgment

We express our gratitude to Zoonoses Laboratory at Centro de Investigaciones Regionales Dr. Hideyo Noguchi (CIR) from Universidad Autónoma de Yucatán for providing the dataset used in this research.

References

[1] Chagas C., Nova tripanozomiaze humana: estudos sobre a morfolojia e o ciclo evolutivo do Schizotrypanum cruzi n. gen., n. sp., ajente etiolojico de nova entidade morbida do homem. Memórias do Instituto Oswaldo Cruz 1909; 1:159-218 (In Portuguese). doi: https://doi.org/10.1590/s0074-02761909000200008.

[2] Sanchez-Patiño N, Toriz-Vazquez A., Hevia-Montiel N., and Perez-Gonzalez J., Convolutional neural networks for chagas' parasite detection in histopathological images. In: IEEE 2021 43rd Annual International Conference of the IEEE Engineering in Medicine Biology Society (EMBC); 2021. pp. 2732-2735. https://doi.org/10.1109/EMBC46164.2021.9629563

[3] Cancino-Faure B., Fisa R., Riera C., Bula I., Girona-Llobera E., and Jimenez-Marco T., Evidence of meaningful levels of Trypanosoma cruzi in platelet concentrates from seropositive blood donors. Transfusion 2015; 55(6): 1249-1255. https://doi.org/10.1111/trf.12989

[4] Filigheddu M.T., Górgolas M., Ramos J.M., Orally-transmitted Chagas disease. Medicina Clínica (English Edition) 2017; 148(3): 125-131. https://doi.org/10.1016/j.medcle.2017.02.007

[5] Luquetti A.O., Tavares S.B., Siriano L.D., Oliveira R.A., Campos D.E., Morais C.A., Oliveira E.C., Congenital transmission of Trypanosoma cruzi in central Brazil. A study of 1,211 individuals born to infected mothers. Memórias do Instituto Oswaldo Cruz 2015; 110 (3): 369-76. https://doi.org/10.1590/0074-02760140410

[6] Dias J.C., Ramos Jr A.N., Gontijo E.D., Luquetti A., Shikanai-Yasuda M.A. et al. 2 nd Brazilian consensus on Chagas disease, 2015. Revista da Sociedade Brasileira de Medicina Tropical 2016; 49: 03-60. https://doi.org/10.1590/0037-8682-0505-2016

[7] Luquetti A.O., Schmuñis G.A., Diagnosis of Trypanosoma cruzi infection. In: Telleria J, Tibayrenc M (editors). American Trypanosomiasis Chagas Disease. 2nd ed. London, UK: Elsevier, 2017, pp. 687-730. https://doi.org/10.4269/ajtmh.17-0141

[8] Ballesteros R.G., Martínez C.I., Jiménez R.T., Antonio C.A., Chagas disease: an overview of diagnosis. Journal of Microbiology Experimentation 2018; 6 (3): 151-157. https://doi.org/10.15406/jmen.2018.06.00207

[9] Anez N., Carrasco H., Parada H., Crisante G., Rojas A. et al. Acute Chagas' disease in western Venezuela: a clinical, seroparasitologic, and epidemiologic study. The American Journal of Tropical Medicine and Hygiene 1999; 60 (2): 215-222. https://doi.org/10.4269/ajtmh.1999.60.215

[10] Kirchhoff L.V., Votava J.R., Ochs D.E., Moser D.R., Comparison of PCR and microscopic methods for detecting Trypanosoma cruzi. Journal of Clinical Microbiology 1996; 34 (5): 1171-1175. https://journals.asm.org/doi/10.1128/jcm.34.5.1171-1175.1996

[11] Storino R., Consenso de enfermedad de Chagas, Topico I: Enfermedad de Chagas con parasitemia evidente. Rev Arg Cardiol 2002; 70(1): 15-39 (In Spanish).

[12] Bern C., Chagas' disease. New England Journal of Medicine 2015; 373(5): 456-466. https://doi.org/10.1056/NEJMra1410150

[13] Gomes Y.M., Lorena V., Luquetti A.O., Diagnosis of Chagas disease: what has been achieved? What remains to be done with regard to diagnosis and follow up studies?. Memórias do Instituto Oswaldo Cruz 2009; 104: 115-121. https://doi.org/10.1590/S0074-02762009000900017

[14] Rajaraman S., Antani S.K., Poostchi M., Silamut K., Hossain M.A. et al. Pre-trained convolutional neural networks as feature extractors toward improved malaria parasite detection in thin blood smear images. PeerJ 2018; 6: e4568. https://doi.org/10.7717/peerj.4568

[15] Górriz M., Aparicio A., Raventós B., Vilaplana V., Sayrol E. et al. Leishmaniasis parasite segmentation and classification using deep learning. In: Articulated Motion and Deformable Objects: 10th International Conference, AMDO 2018; Palma de Mallorca, Spain; 2018. pp. 53-62. https://doi.org/10.1007/978-3-319-94544-6_6

[16] Rosado L., Da Costa J.M., Elias D., Cardoso J.S., Mobile-based analysis of malaria-infected thin blood smears: automated species and life cycle stage determination. Sensors 2017; 17 (10): 2167. https://doi.org/10.3390/s17102167

[17] Oliveira A.D., Prats C., Espasa M., Serrat F.Z., Sales C.M. et al. The malaria system microapp: a new, mobile device-based tool for malaria diagnosis. JMIR Research Protocols 2017; 6 (4): e6758. https://doi.org/10.2196/resprot.6758

[18] Latif J., Xiao C., Imran A., Tu S., Medical imaging using machine learning and deep learning algorithms: a review. In: 2nd International Conference on Computing, Mathematics and Engineering Technologies (iCoMET); Sukkur, Pakistan; 2019. pp. 1-5. https://doi.org/10.1109/ICOMET.2019.8673502

[19] Alsheref F.K., Gomaa W.H., Blood diseases detection using classical machine learning algorithms. International Journal of Advanced Computer Science and Applications 2019; 10 (7). https://doi.org/10.14569/IJACSA.2019.0100712

[20] Soberanis-Mukul R., Uc-Cetina V., Brito-Loeza C., Ruiz-Piña H., An automatic algorithm for the detection of Trypanosoma cruzi parasites in blood sample images. Computer Methods and Programs in Biomedicine 2013; 112 (3): 633-639. https://doi.org/10.1016/j.cmpb.2013.07.013

[21] Soberanis-Mukul R. Algoritmos de segmentación de Trypanosoma cruzi en imágenes de muestras sanguineas. MSc Thesis, Universidad Autónoma de Yucatán, Mérida, México, 2013 (in Spanish).

[22] Peterson L.E., K-nearest neighbor. Scholarpedia 2009; 4 (2): 1883. https://doi.org/10.4249/scholarpedia.1883

[23] Uc-Cetina V., Brito-Loeza C., Ruiz-Piña H., Chagas parasite detection in blood images using AdaBoost. Computational and Mathematical Methods in Medicine 2015; 2015: 139681. https://doi.org/10.1155/2015/139681

[24] Pereira A.C., Pyrrho A.S., Vanzan D., Mazza L., Gomes J., Deep Convolutional Neural Network applied to Chagas Disease Parasitemia Assessment. Anais do 14. Congresso Brasileiro de Inteligência Computacional 2020. pp. 1-8. https://doi.org/10.21528/CBIC2019-119

[25] Ojeda-Pat A., Martin-Gonzalez A., Soberanis-Mukul R., Convolutional neural network U-Net for Trypanosoma cruzi segmentation. In: Third International Symposium on Intelligent Computing Systems (ISICS 2020); Sharjah, United Arab Emirates; 2020. pp. 118-131. https://doi.org/10.1007/978-3-030-43364-2_11

[26] Morais M.C., Silva D., Milagre M.M., de Oliveira M.T., Pereira T. et al. Automatic detection of the parasite Trypanosoma cruzi in blood smears using a machine learning approach applied to mobile phone images. PeerJ 2022; 10: e13470. https://doi.org/10.7717/peerj.13470

[27] Ojeda-Pat A., Martin-Gonzalez A., Brito-Loeza C., Ruiz-Piña H., Ruz-Suarez D. Effective residual convolutional neural network for Chagas disease parasite segmentation. Medical Biological Engineering Computing 2022; 60 (4): 1099-1110. https://doi.org/10.1007/s11517-022-02537-9

[28] Huang G., Liu Z., Van Der Maaten L., Weinberger K.Q., Densely connected convolutional networks. In: IEEE Conference on Computer Vision and Pattern Recognition (CVPR); Honolulu, HI, USA; 2017. pp. 4700-4708. https://doi.org/10.1109/CVPR.2017.243

[29] Pihur V., Datta S., Datta S., Weighted rank aggregation of cluster validation measures: a Monte Carlo cross-entropy approach. Bioinformatics 2007; 23 (13): 1607-1615. https://doi.org/10.1093/bioinformatics/btm158

[30] Polak M., Zhang H., Pi M., An evaluation metric for image segmentation of multiple objects. Image and Vision Computing 2009; 27 (8): 1223-1227. https://doi.org/10.1016/j.imavis.2008.09.008

[31] Sudre C.H., Li W., Vercauteren T, Ourselin S, Cardoso MJ. Generalised dice overlap as a deep learning loss function for highly unbalanced segmentations. In: Deep Learning in Medical Image Analysis and Multimodal Learning for Clinical Decision Support; Québec City, QC, Canada; 2017. pp. 240-248. https://doi.org/10.1007/978-3-319-67558-9_28

[32] Lin T.Y., Goyal P., Girshick R., He K., Dollár P., Focal loss for dense object detection. In: IEEE International Conference on Computer Vision (ICCV); Venice, Italy; 2017. pp. 2980-2988. https://doi.org/10.1109/ICCV.2017.324